International Journal of the Physical Sciences Vol. 6(33), pp. 7490 - 7504, 9 December, 2011
Available online at http://www.academicjournals.org/IJPS
DOI: 10.5897/IJPS11.760
ISSN 1992 - 1950 ©2011 Academic Journals

Full Length Research Paper

Investigation of nuclear magnetic resonance (NMR) shielding tensors of $B_5N_5C_8H_{18}$ cluster as a novel material for nano drug delivery

M. Monajjemi[1]*, H. Aghaie[1], P. Ardalan[1#] and F. Mollaamin[2]

[1]Department of Chemistry, Science and Research Branch, Islamic Azad University, Tehran, Iran.
[2]Department of Chemistry, Qom Branch, Islamic Azad University, Qom, Iran.

Accepted 20 June, 2011

The interaction of the penicillin molecule inside of the $B_5N_5C_8H_{18}$ have been investigated with density functional theory using HF and B3LYP method and 6-31G, 6-31G and 6-311G** basis sets. We also analyze the electronic structure and charge Mulliken population for the energetically most favorable complexes. Our results indicate penicillin can form stable bindings with $B_5N_5C_8H_{18}$ via the nitrogen active site. Also the NMR shielding tensors have been investigated. The same study performed for cefalexin and we found that cefalexin can form stable bindings with $B_5N_5C_8H_{18}$ via the nitrogen active site. Thus, we arrive at the prediction that the $B_5N_5C_8H_{18}$ can be implemented as a novel material for drug delivery applications.**

Key words: $B_5N_5C_8H_{18}$, Cefalexin, DFT, NMR, drug delivery.

INTRODUCTION

Heterofullerenes became a subject of research interest soon after the establishment of fullerene research itself (Curl and Smalley, 1988; Kroto, 1988; Monajjemi et al., 2011). The fullerenes containing boron and/or nitrogen atoms represent one distinguished class, though other elements have been combined with the fullerenes too (Locke et al., 1994; Behrman et al., 1994; Kaxiras et al., 1994). Boron nitride (BN) is a synthetic III-V compound with extraordinary mechanical, thermal, electrical, optical, and chemical properties widely applied for technological purposes (Curl and Smalley, 1988).

Since BN units are isoelectronic with hexagonal BN possessing a graphene-like layered structure, BN becomes the natural candidate to form heterofullerenes, which results in a certain isomorphism. BN crystalline samples were synthesized at room temperature and atmospheric pressure as structures containing hexagonal sp^2-bonded sheets isomorphic with grapheme (Haubner et al., 2002). BN nanomaterials are expected in application due to the good stability at high temperatures with high electronic insulation in air (Naruhiro and Takeo, 2004). Despite the carbon nanotubes, BN nanotubes are constant band gap materials and thus provide an attractive opportunity for practical applications (Moon and Hwang, 2004). The wide range of their electronic properties from metallic to wide-gap semiconductors, depending on their chemical composition, makes them suitable candidates for nanosize electronic devices (Monajjemi et al., 2008; Mollaamin et al., 2011). Due to the similarity between B-N and C-C units, a lot of effort has been devoted to BN fullerene-like materials in recent years, which have excellent properties such as heat resistance, insulation, and structural stability (Monajjemi et al., 2010a, b; Nirmala and Kolandaivel, 2007).

Several studies have been made on BN nanomaterials such as BN nanotubes, BN nanocapsules, and BN clusters since they have excellent properties such as heat resistance in air and insulation, and these nano-particles are expected to be useful as electronic devices, high heat resistance semiconductors, and insulator lubricants (Monajjemi et al., 2009; Golberg et al., 1998; Szakacs and Mezey, 2008; Takeo et al., 2004). From the experimental standard formation enthalpy, the energies of hybridized sp^2 and sp3 B-N bonds are known to be stronger in comparison with those of B-B and N-N bonds, namely, 4.00, 2.32, and 2.11 eV, respectively (Pokropivny et al., 2000). Along with the experimental

*Corresponding author. E-mail: m_monajjemi@yahoo.com.
#Ph.D Student

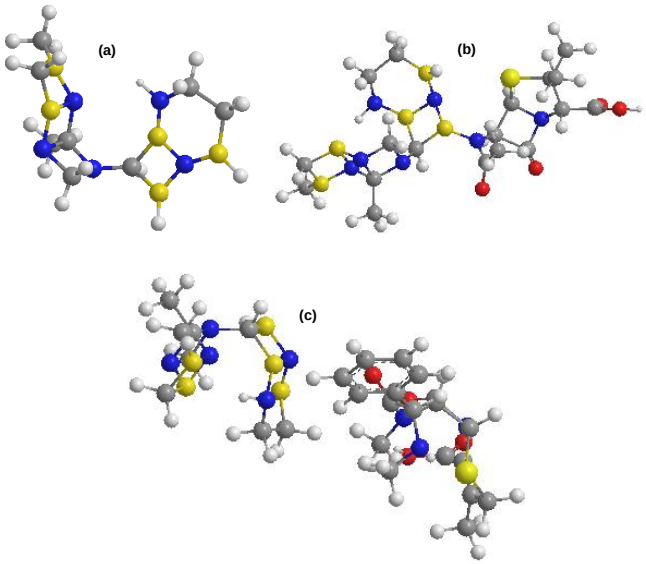

Figure 1. The optimized a) $B_5N_5C_8H_{18}$ cluster b) $B_5N_5C_8H_{18}$ inside penicillin cluster and c) $B_5N_5C_8H_{18}$ inside cefalexin cluster.

efforts, extensive theoretical studies have also been carried out on BN fullerenes to understand their relative stability and size dependence of the properties (Loiseau et al., 1998; Azevedo, 2006; Monajjemi et al., 2010a, b). Several investigations have dealt with the possibility of inorganic analogues of the fullerene cages that would be constructed entirely of BN pairs (Kar et al., 2003; Tang et., 1993; Seifert et al., 1997, Sun et al., 1995). Since the thermodynamic conditions for growth of BN nanotubes from nuclei are still not well-defined, comprehensive theoretical simulations on these nanotubes continue to attract enhanced attention, and the lack of theoretical thermodynamic data precludes a more detailed analysis (Zhukovskii et al., 2009). These nanotubes are found to be chiral or nonchiral; however, a preference toward the armchair and zigzag configurations is suggested. Electron energy loss spectroscopy yields a B/N ratio of approximately 1 and a perfect chemical homogeneity (Deepak et al., 2002). This paper focuses on the $B_5N_5C_8H_{18}$ cluster as a new material for drug delivery.

METHODOLOGY

Computational details

Calculations were performed using an all-electron linear combination of atomic orbitals Hatree–Fock (HF) and density functional theory (DFT) calculations using the Gaussian 03 package. The optimizations of antibiotics and $B_5N_5C_8H_{18}$ are carried out including exchange and correlation contributions using Beckės three parameter hybrid and Lee-Yang-Parr (LYP) correlation [B3LYP]; including both local and non local terms. We have geometric optimization calculation at the HF/6-31G, HF/6-31G**, HF/6-311G**. We have also performed a geometric optimization calculation at the B3LYP/6-31G, B3LYP/6-31G** and B3LYP/6-31G** level.

The NMR isotropic shielding constants were calculated using the standard GIAO (Gauge-Independent Atomic Orbital) approach of Gaussian 03 program package.

a) The isotropic value σiso of the shielding tensor which can be defined as:

$$\sigma_{iso} = \frac{1}{3}(\sigma_{11} + \sigma_{22} + \sigma_{33})$$

b) The anisotropy parameter (Δσ) defined as:

$$\text{If } |\sigma_{11} - \sigma_{iso}| \geq |\sigma_{33} - \sigma_{iso}| \quad \Delta\sigma = \sigma_{11} - \frac{\sigma_{22} + \sigma_{33}}{2}$$

$$\text{If } |\sigma_{11} - \sigma_{iso}| \leq |\sigma_{33} - \sigma_{iso}| \quad \Delta\sigma = \sigma_{33} - \frac{\sigma_{22} + \sigma_{11}}{2}$$

and

c) The asymmetry parameter (η) which is given by:

$$\text{If } |\sigma_{11} - \sigma_{iso}| \geq |\sigma_{33} - \sigma_{iso}| \quad \eta = \frac{\sigma_{22} - \sigma_{33}}{\delta}$$

$$\text{If } |\sigma_{11} - \sigma_{iso}| \leq |\sigma_{33} - \sigma_{iso}| \quad \eta = \frac{\sigma_{22} - \sigma_{11}}{\delta}$$

RESULTS AND DISCUSSION

We studied $B_5N_5C_8H_{18}$ cluster as a novel material for drug delivery (Figure 1). Before and after connecting the anti-biotics to $B_5N_5C_8H_{18}$, NMR calculations were performed in electric field of charges. NMR parameters are listed in Tables 1 to 3 in different levels and different basis sets.

σ_{iso}, σ_{aniso}, $\Delta\sigma$, δ and η curves versus atomic charges

Table 1. Nuclear magnetic resonance parameters of nitrogen, bohr, carbon and hydrogen atoms in $B_5N_5C_8H_{18}$ at the different levels.

	Atom	σ_{iso}	σ_{aniso}	Detminan (NMR)	Distance matrix	ΔE	δ	η	Δσ	Dipole orientation	Atomic charge
HF/6-311G**	B(1)	71.339	55.0844	271770.3251	-8.67485E+11	-713.9823119	-36.0498	-0.981328607	55.08435	2.2123	0.387581
	N(2)	40.9141	352.1099	908300.9883			-167.6679	-0.599970537	352.11		-0.246422
	B(3)	50.4739	92.7906	-4224.414708			-51.5349	-0.799640632	92.7906		0.234636
	N(4)	-26.7538	277.6674	2053130.068			-133.2069	-0.61034526	277.6674		-0.326638
	C(5)	58.3468	57.2294	149280.2848			-22.8462	-0.330006741	57.2294		0.202448
	N(6)	177.0685	120.3381	4818678.789			-59.0358	-0.641072027	120.3381		-0.389498
	B(7)	49.9521	92.7553	-34488.43859			-57.1566	-0.918116193	92.7553		0.315294
	N(8)	162.3581	53.179	3800026. 984			-59.482	0.192048015	-89.223		-0.420412
	C(9)	159.1911	21.9121	4005948.896			-13.0421	-0.87993498	21.9121		-0.365365
	B(10)	47.2762	92.1485	-33461.75494			-54.886	-0.880727326	92.1485		0.193477
	C(11)	135.1987	55.0446	2348081.285			-23.6559	-0.448746402	55.04455		-0.195177
	C(12)	156.8929	39.8818	3770175.56			-22.5592	-0.82141654	39.88185		-0.179611
	C(13)	179.4742	16.5152	5745745.287			-16.2374	0.35614692	-24.35605		-0.463998
	C(14)	139.9692	42.6442	2652087.622			-23.1209	-0.770402536	42.6442		-0.085183
	C(15)	159.3001	26.9515	3969700.379			-24.2592	0.481306061	-36.38885		-0.454436
	B(16)	55.0599	79.8852	51629.8684			-45.2616	-0.823360199	79.8851		0.321805
	N(17)	131.0717	83.3857	1971180.183			-72.7924	0.527369616	-109.18865		-0.369803
	C(18)	108.6623	53.3352	1192205.27			-20.0825	-0.229458484	53.33525		0.051303
B3LYP/6-31G	B(1)	93.9359	46.3114	733235.8956	-8.67485E+11	-708.8603316	-33.2479	0.857215042	-49.8718	2.4704	0.979824
	N(2)	90.0569	317.1431	-801792.7611			-159.6575	-0.675735872	317.14315		-1.112541
	B(3)	79.163	80.555	327945.5187			-43.4142	-0.76300381	80.555		0.721909
	N(4)	20.8062	255.5652	502858.8862			-129.4654	-0.683997423	255.5651		-0.891237
	C(5)	94.2551	46.0343	778316.235			-19.2142	-0.402769826	46.03435		0.451311
	N(6)	217.8687	126.574	9317977.508			-56.6285	-0.509889896	126.57395		-0.734899
	B(7)	75.7464	81.9133	203315.9643			-56.0944	0.947033929	-84.14165		0.832838
	N(8)	203.5855	52.2952	7795754.837			-62.0444	0.123824229	-93.0665		-0.966665
	C(9)	187.512	16.931	6573777.856			-9.4305	-0.803117544	16.931		-0.62567
	B(10)	74.6728	76.2827	254894.2489			-45.6574	-0.886158651	76.28265		0.688988
	C(11)	167.0391	48.8332	4537392.617			-18.1632	-0.2076176	48.8332		-0.44107
	C(12)	179.521	37.2242	5696058.119			-20.0805	-0.764169219	37.22415		-0.425061
	C(13)	200.3241	14.1047	8004466.792			-15.1693	0.239753977	-22.75395		-0.752583
	C(14)	171.8609	35.9565	4997609.353			-18.8057	-0.725333277	35.9565		-0.053262
	C(15)	185.8349	20.4583	6359214.593			-20.3482	0.340546093	-30.52235		-0.808434
	B(16)	77.8694	67.898	330895.1228			-42.5165	-0.935347453	67.89805		0.916932

Table 1. Cont'd

	N(17)	160.7095	88.5067	3853515.443			-65.5224	0.801049717	-98.28355		-0.722523
	C(18)	142.0558	56.1034	2726328.547			-24.0451	-0.444493889	56.10345		0.124685
	B(1)	90.525	44.7348	659377.8885			-30.9497	0.927198002	-46.42465		0.632036
	N(2)	97.0537	308.8633	-727607.5484			-152.4084	-0.648966199	308.86325		-0.629544
	B(3)	75.43	77.13	283595.4798			-41.2197	-0.752538228	77.13		0.48
	N(4)	32.5506	256.6188	286391.2308			-128.77	-0.671435893	256.6188		-0.678016
	C(5)	95.7672	45.6706	818900.8112			-19.2998	-0.422413704	45.67055		0.547114
	N(6)	220.2753	117.5848	9782676.855			-53.4933	-0.534582836	117.5848		-0.675544
	B(7)	73.046	80.1454	199385.5915			-51.1279	-0.954969791	80.1454		0.576434
	N(8)	203.8123	45.0641	7964508.618			-55.1816	0.088868391	-82.77235		-0.720248
	C(9)	183.0484	16.3564	6115329.829			-9.4198	-0.842406421	16.35635		-0.441551
B3LYP/6-31G**	B(10)	72.3919	74.4889	240378.6302	-8.67485E+11	-709.2088833	-42.2248	-0.823928118	74.4889	2.1768	0.427204
	C(11)	164.6599	49.8192	4337489.853			-19.3667	-0.285051144	49.81925		-0.212421
	C(12)	175.5921	33.7101	5338857.605			-19.359	-0.839123922	33.7101		-0.309594
	C(13)	196.3073	12.7602	7540110.547			-13.0683	0.301906139	-19.6024		-0.551841
	C(14)	165.2389	35.3719	4439077.429			-18.259	-0.708510871	35.37195		0.001601
	C(15)	183.5508	21.1287	6129271.138			-19.4783	0.44631205	-29.2174		-0.570949
	B(16)	75.9556	65.4684	314482.5288			-39.5997	-0.897827509	65.46845		0.654829
	N(17)	176.7877	77.9045	5254247.805			-60.5737	0.714816826	-90.86055		-0.697552
	C(18)	138.3357	48.5574	2546862.092			-18.6544	-0.264666781	48.5574		0.197172
	B(1)	83.3029	48.4224	485319.4617			-34.3425	0.879979617	-51.51375		0.532663
	N(2)	76.9321	324.0219	-503804.0862			-159.8251	-0.648430691	324.02195		-0.411984
	B(3)	67.682	81.789	169032.2261			-43.246	-0.739166628	81.789		0.318244
	N(4)	8.1597	269.4194	920002.4456			-137.3938	-0.692713936	269.4194		-0.510542
	C(5)	86.5758	51.0135	584118.5551			-20.681	-0.355548571	51.01345		0.360685
	N(6)	207.4518	131.7445	7888531.942			-58.0918	-0.48808782	131.74455		-0.538949
	B(7)	65.2205	85.0981	87673.56453			-54.1857	-0.953007897	85.0981		0.45146
B3LYP/6-311G**	N(8)	190.5332	46.7711	6381426.718	-8.67485E+11	-709.3375859	-58.5693	0.064747231	-87.8539	2.0748	-0.546939
	C(9)	174.0622	18.4208	5252787.23			-10.29	-0.806550049	18.4208		-0.379404
	B(10)	65.1056	81.0485	134915.216			-45.1347	-0.802863429	81.0485		0.288286
	C(11)	156.0797	51.5049	3675095.458			-19.7876	-0.264746609	51.50485		-0.216334
	C(12)	167.8563	35.8143	4648704.56			-20.5798	-0.839823516	35.8143		-0.133341
	C(13)	188.9642	15.299	6717367.214			-14.5878	0.398325998	-21.88175		-0.455233
	C(14)	156.6456	35.9258	3772597.722			-18.6217	-0.71383386	35.9258		0.010945
	C(15)	175.7067	23.6701	5361245.59			-21.2386	0.48597836	-31.85795		-0.510154

Table 1. Cont'd

B(16)	68.8357	71.3229	195008.4996	-42.8971	-0.891566097	71.3229	0.470667
N(17)	162.233	87.4383	3926613.881	-67.2494	0.733611006	-100.87415	-0.513486
C(18)	129.0664	49.5839	2053505.506	-18.9028	-0.251269653	49.58395	0.166259

Table 2. Nuclear magnetic resonance parameters of Penicillin cluster inside of the $B_5N_5C_8H_{18}$ at the different levels.

	Atom	σ_{iso}	σ_{aniso}	Detminan (NMR)	∆E(J)	δ	η	Δσ	Dipole orientation	Atomic charge
B3LYP/6-31G	B(1)	56.446	64.3948	98853.99391	-5009.629	-39.1607	-0.903753	64.3947	5.1544	0.595231
	N(2)	7.5448	273.9685	-1145400.206		-204.4628	0.7865905	-306.6942		-0.746352
	B(3)	60.0118	102.2879	-13278.0525		-62.6823	-0.912101	102.2879		0.463841
	N(4)	-35.3143	399.6306	1970384.781		-273.272	0.9498555	-409.9081		-0.570803
	C(5)	88.4038	47.8615	630410.1603		-22.9725	-0.611057	47.86145		0.241716
	N(6)	182.5767	101.6527	5592719.157		-49.6182	-0.634199	101.6527		-0.491544
	B(7)	22.7361	142.1503	-125890.3435		-88.4319	-0.928363	142.15025		0.590474
	N(8)	144.613	78.0799	2607946.773		-66.3908	0.5680847	-99.5862		-0.643099
	C(9)	169.7	19.6109	4867988.148		-9.8013	-0.666106	19.61095		-0.428384
	B(10)	47.5347	85.0297	-10410.63388		-52.0943	-0.911848	85.02975		0.763825
	C(11)	140.7531	21.0486	2768179.923		-10.7057	-0.689268	21.04855		-0.263564
	C(12)	166.3879	36.0793	4516279.501		-23.5563	-0.978919	36.07935		-0.374427
	C(13)	168.6536	22.4601	4720965.586		-24.6022	0.2172407	-36.9033		-0.578323
	C(14)	148.2957	42.9865	3097926.683		-36.2203	0.5824054	-54.33055		-0.161046
	C(15)	152.554	32.3557	3475336.48		-24.3969	0.7682943	-36.5953		-0.608057
	B(16)	33.0517	110.1145	-139111.5463		-74.0921	0.9815783	-111.1381		0.558334
	N(17)	62.2654	186.4204	-256214.0411		-139.4093	0.7829549	-209.114		-0.47359
	C(18)	131.3383	38.7514	2206955.075		-15.4571	-0.328645	38.75145		0.033454
	C(19)	121.1326	55.5839	1623340.244		-35.8175	-0.965425	55.58385		-0.259977
	N(20)	55.6594	101.5419	214668.7322		-45.6308	-0.516471	101.5419		-0.430786
	C(21)	117.5277	31.3995	1495705.14		-36.8184	0.1370972	-55.22765		-0.011013
	C(22)	130.9758	49.063	2080853.643		-38.9597	0.6791017	-58.4395		-0.314155
	S(23)	435.7665	378.6156	61169314.8		-211.5054	-0.8066	378.61565		0.364183
	C(24)	92.8846	52.202	599123.5894		-54.4999	0.2771143	-81.74995		-0.015855
	C(25)	13.3782	124.7299	-356074.2312		-111.9751	0.4852097	-167.9626		0.433238
	O(26)	-393.9891	986.4081	127516887.2		-520.9665	-0.73772	986.40805		-0.30826
	N(27)	98.4296	75.444	457676.085		-88.8006	0.1327863	-133.201		-0.651304
	C(28)	157.4818	40.5304	3814485.057		-21.0745	-0.717868	40.53045		-0.376944

Table 2. Cont'd

	C(29)	159.9323	40.2989	3989519.427		-24.0009	-0.880625	40.2989	-0.391766
	C(30)	9.581	122.8421	-328139.2174		-110.4113	0.4834487	-165.6169	0.430008
	C(31)	155.3664	44.8436	3653239.704		-19.6244	-0.476606	44.84365	-0.45831
	O(32)	-342.7353	952.2486	113077619.8		-535.1351	-0.813697	952.24865	-0.334509
	C(33)	19.7829	91.8298	-461860.8398		-108.0194	0.1334973	-162.0292	0.5205
	O(34)	-166.3746	647.0505	37074964.64		-281.2616	-0.466314	647.0505	-0.370315
	O(35)	98.8177	237.382	-1687192.404		-173.7909	0.8212076	-260.6864	-0.577683
	B(1)	53.6397	63.7974	83936.32311		-37.5124	-0.866199	63.7974	0.410821
	N(2)	13.9548	264.7252	-1311434.553		-198.9498	0.7741506	-298.4247	-0.498072
	B(3)	57.4346	100.2332	-14018.38557		-60.5531	-0.896473	100.2332	0.331444
	N(4)	-31.1023	420.1064	2199147.946		-282.1709	0.9851158	-423.2564	-0.481197
	C(5)	90.3528	48.313	671011.3823		-24.1383	-0.66566	48.31305	0.411148
	N(6)	187.653	95.8372	6173911.571		-41.2403	-0.450753	95.8372	-0.503713
	B(7)	21.4992	139.8517	-75518.07328		-82.5751	-0.870913	139.85175	0.415044
	N(8)	150.249	73.1268	2990238.576		-63.1656	0.5435981	-94.74845	-0.53672
	C(9)	166.8747	18.7047	4630817.604		-8.9269	-0.60311	18.70475	-0.305436
	B(10)	44.2563	85.9686	-28662.15663		-53.5	-0.92874	85.9687	0.497563
	C(11)	138.7995	18.9903	2657690.874		-10.2461	-0.764388	18.9903	-0.071202
	C(12)	163.9713	33.3654	4327835.992		-23.0591	0.9292687	-34.58865	-0.312461
	C(13)	167.6565	20.9388	4653943.969		-21.7083	0.2860703	-32.56235	-0.439924
	C(14)	143.6137	42.3466	2806421.49		-35.7808	0.5780027	-53.6712	-0.078601
	C(15)	150.3466	30.9127	3319088.094		-26.4157	0.5603221	-39.62355	-0.434747
	B(16)	29.1448	115.6924	-93864.83033		-70.7439	-0.909755	115.6924	0.434815
	N(17)	72.2813	200.3651	-384691.39		-142.1207	0.8797649	-213.181	-0.471234
	C(18)	128.3208	34.4293	2065190.034		-16.8151	-0.634989	34.4293	0.111816
	C(19)	119.4616	55.7777	1564262.311		-33.5614	-0.892025	55.7778	-0.065473
B3LYP/6-31G**	N(20)	61.1618	97.3125	205841.2075		-43.4356	-0.506412	97.31245	-0.420498
	C(21)	115.7924	31.1022	1432630.654		-35.9929	0.1521606	-53.98935	0.01324
	C(22)	128.6545	47.584	1966043.035	-5011.127	-39.0811	0.6234292	-58.62165	4.6032 -0.153575
	S(23)	406.9668	408.4926	45545911.92		-217.869	-0.750036	408.4926	0.136345
	C(24)	91.5055	52.7538	580963.4062		-52.9624	0.3280818	-79.4436	0.001643
	C(25)	12.7761	118.8589	-243109.9473		-101.0543	0.5682509	-151.5815	0.478458
	O(26)	-345.2228	919.7861	105500046.9		-478.7112	-0.71908	919.78605	-0.363935
	N(27)	101.2446	70.4452	581555.9087		-85.801	0.0947064	-128.7016	-0.499231
	C(28)	154.8885	37.3918	3638705.767		-19.6942	-0.734252	37.39175	-0.30331
	C(29)	157.3246	37.8345	3803851.291		-23.2007	-0.912835	37.8345	-0.313695
	C(30)	10.5573	114.0098	-275315.7182		-102.3233	0.4856157	-153.4849	0.488347
	C(31)	153.7015	41.1181	3546993.326		-19.9527	-0.626146	41.11815	-0.377709
	O(32)	-288.4577	869.581	87198670.17		-474.7179	-0.77881	869.58105	-0.384937
	C(33)	22.5571	83.8307	-405536.7015		-101.0976	0.1056078	-151.6464	0.597229
	O(34)	-125.2493	591.1371	26784695.12		-251.0061	-0.429953	591.13705	-0.427407
	O(35)	118.3752	223.6213	-892927.0538		-158.3628	0.8827768	-237.5441	-0.530699
	B(1)	41.287	70.4191	9044.044697		-41.3866	-0.865671	70.4191	0.329586
	N(2)	-14.1765	285.1995	-443879.8734		-213.7736	0.7788258	-320.6604	-0.355355
	B(3)	43.1581	110.2176	-89176.80689		-65.9788	-0.886335	110.21755	0.213885
	N(4)	-64.2271	455.0969	5426559.491		-305.1313	0.9886383	-457.6971	-0.352731
	C(5)	77.7697	53.3766	399029.7207		-27.9471	-0.726727	53.37655	0.177236
	N(6)	173.3487	105.9379	4725770.414		-47.4339	-0.51108	105.93785	-0.372507
	B(7)	5.6101	154.7495	56646.87623		-91.3448	-0.870584	154.74945	0.334756
	N(8)	133.695	78.0066	2003718.818		-66.6272	0.5610561	-99.9408	-0.367574

Table 2. Cont'd

	C(9)	156.4882	21.049	3811636.478	-11.2049	-0.747628	21.04895	-0.333666
	B(10)	30.5296	96.6764	-61239.42018	-59.6994	-0.92041	96.67645	0.483213
	C(11)	127.0805	18.8896	2035885.36	-11.1585	-0.871434	18.88955	-0.172905
	C(12)	154.8695	37.7988	3617517.009	-25.8188	0.952004	-38.7283	-0.212463
	C(13)	157.5556	25.7579	3833116.844	-25.3217	0.356307	-37.98245	-0.421209
	C(14)	132.2081	47.4482	2138410.197	-38.8026	0.6304114	-58.2039	-0.143079
	C(15)	138.0518	34.8941	2537163.653	-29.7305	0.5649081	-44.5957	-0.436326
	B(16)	14.9521	129.7526	-33240.11861	-77.6552	-0.886081	129.7526	0.297808
	N(17)	47.3035	215.4939	-293114.4377	-153.8947	0.8670247	-230.8421	-0.334306
	C(18)	115.8433	36.9117	1504017.512	-19.4168	-0.732659	36.91165	0.030853
	C(19)	106.5135	58.6877	1076930.457	-33.8972	-0.845772	58.68765	-0.122519
	N(20)	35.5015	107.7428	67160.9689	-44.5025	-0.385965	107.7428	-0.304717
	C(21)	104.2576	33.5467	999070.2221	-39.7201	0.1261049	-59.58015	0.021397
	C(22)	116.6663	51.7263	1417734.026	-41.6132	0.6573659	-62.41985	-0.443296
	S(23)	345.704	429.2927	21023701.73	-232.7667	-0.770464	429.29275	0.185818
	C(24)	76.8204	54.5887	281875.6433	-55.8599	0.3029902	-83.7899	-0.03769
	C(25)	-7.2098	128.4207	-163582.1996	-113.7187	0.5057119	-170.5781	0.307057
	O(26)	-411.0858	989.121	127345925.6	-512.6709	-0.713767	989.121	-0.246317
	N(27)	79.3735	75.3647	10431.51877	-95.0957	0.0566861	-142.6436	-0.415956
	C(28)	144.8816	42.1636	2948517.147	-22.9471	-0.775052	42.1636	-0.223659
	C(29)	147.7537	43.204	3118169.43	-25.8158	-0.884303	43.204	-0.237479
	C(30)	-10.189	123.8139	-197251.8036	-116.1365	0.4214765	-174.2047	0.249425
	C(31)	142.9918	45.6407	2833003.953	-20.8182	-0.538438	45.64075	-0.300407
	O(32)	-352.3394	933.8497	107944069.9	-510.7871	-0.781163	933.8497	-0.263528
	C(33)	0.8106	90.7396	-354036.5931	-112.7635	0.072919	-169.1453	0.395018
	O(34)	-173.4067	630.6696	35048884.5	-267.4773	-0.428104	630.6696	-0.306611
	O(35)	94.83	245.4916	-1501985.842	-167.1257	0.958539	-250.6886	-0.377747

Table 3. Nuclear magnetic resonance parameters of Cefalexin cluster inside of the $B_5N_5C_8H_{18}$ at the different levels.

	Atom	σ_{iso}	σ_{aniso}	Detminan (NMR)	∆E(J)	δ	η	Δσ	Dipole orientation	Atomic charge
B3LYP/6-31G	B(1)	68.4903	69.1718	232644.6568	-5966.515	-31.4999	-0.536043	69.17185	6.7047	0.656489
	N(2)	-30.343	385.5816	4364698.605		-201.126	-0.721924	385.58155		-0.670821
	B(3)	60.5393	87.7131	54111.72392		-52.3817	-0.883665	87.71315		0.445861
	N(4)	-57.4522	306.3997	2219488.029		-201.7934	-0.987745	306.3997		-0.565212
	C(5)	87.3609	43.1577	610319.1473		-23.2335	-0.761629	43.15765		0.218784
	N(6)	173.9529	104.4781	4738450.815		-41.2441	-0.311223	104.47815		-0.47319
	B(7)	46.0611	109.5266	-50939.67877		-59.9364	-0.781745	109.5266		0.597706
	N(8)	157.3794	74.7354	3542733.965		-51.2794	0.9432228	-76.91905		-0.681536
	C(9)	165.3173	23.6772	4484316.939		-12.8343	-0.770116	23.67715		-0.441832
	B(10)	48.9009	100.1204	-34949.62919		-58.2667	-0.854457	100.1204		0.424223
	C(11)	138.2314	38.9962	2564505.086		-25.9581	-0.998478	38.9962		-0.28436
	C(12)	164.69	30.9565	4389857.615		-22.5094	0.8337006	-33.76405		-0.355985
	C(13)	178.7742	19.4076	5660848.468		-19.5211	0.3255759	-29.2817		-0.60161
	C(14)	149.4618	42.3789	3214112.108		-30.4083	0.8582196	-45.6124		-0.159467
	C(15)	149.2172	27.9744	3189073.09		-34.7916	0.0720777	-52.18735		-0.619151
	B(16)	42.6566	91.2207	-104249.4308		-64.5852	0.8832116	-96.8777		0.565979
	N(17)	87.6257	161.3396	46667.92826		-128.215	0.6778021	-192.3226		-0.475919
	C(18)	132.4175	39.0396	2261379.77		-15.8219	-0.355046	39.03955		0.040491
	C(19)	65.1059	167.954	-271776.8483		-96.2154	-0.836263	167.954		-0.153978

Table 3. Cont'd

	C(20)	65.3295	166.5894	-303637.3025		-98.1762	-0.868774	166.58935		-0.125705
	C(21)	65.2136	163.2866	-299956.7387		-97.3199	-0.881445	163.28655		-0.13305
	C(22)	63.4765	150.043	-282342.4237		-93.6847	-0.932285	150.043		-0.156956
	C(23)	58.0764	167.0231	-211034.6515		-91.0068	-0.776479	167.02305		0.143333
	C(24)	59.3923	169.201	-223830.8865		-92.5947	-0.781781	169.201		-0.133526
	C(25)	115.1753	24.1352	1508936.346		-12.4021	-0.702631	24.13525		-0.172338
	C(26)	-8.7729	137.3458	-95507.3054		-114.1691	0.6040041	-171.2536		0.434042
	N(27)	188.8303	109.4027	6056910.252		-46.0227	-0.415234	109.4027		-0.545945
	C(28)	98.6598	48.4053	736573.4288		-51.9934	0.2413191	-77.9902		-0.030333
	C(29)	-2.7745	109.6101	-121101.0047		-97.7862	0.4945544	-146.6793		0.481631
	N(30)	-0.7263	241.7513	-1859249.036		-231.0869	0.3948653	-346.6303		-0.508154
	C(31)	130.8561	32.8869	2186224.469		-21.2298	-0.967268	32.88695		-0.249632
	C(32)	35.8305	84.4723	-318853.2844		-87.3467	0.2894568	-131.0201		0.131964
	C(33)	76.66	119.3949	106550.2584		-65.9621	-0.793298	119.3949		0.097167
	C(34)	159.8697	24.4229	4054774.468		-12.6051	-0.708309	24.42285		-0.606075
	S(35)	597.2326	144.6702	212574202.5		-60.8447	-0.414871	144.67015		0.35521
	C(36)	167.9892	37.2746	4643656.529		-23.7689	-0.954525	37.2746		-0.464962
	C(37)	24.573	101.8253	-486064.4442		-107.1738	0.2667937	-160.7608		0.461319
	O(38)	-226.4011	704.2193	48353354.91		-346.6048	-0.645491	704.2193		-0.326976
	O(39)	78.3326	186.4429	-2240169.289		-178.7414	0.3907836	-268.112		-0.547079
	O(40)	-269.3962	755.3328	60194540.3		-371.5603	-0.644755	755.33285		-0.368616
	O(41)	-449.9816	1131.697	183785277		-660.8723	-0.858381	1131.697		-0.311351
	N(42)	214.8101	57.9711	9692153.593		-23.7674	-0.373928	57.97115		-0.530523
	C(43)	155.7657	29.911	3737993.226		-16.7385	-0.808693	29.91095		-0.240282
	C(44)	155.6646	35.1409	3694300.701		-21.4552	-0.908088	35.1409		-0.275544
	B(1)	65.7518	69.052	203090.1718		-29.6979	-0.4499	69.05205		0.463025
	N(2)	-24.9193	376.0367	3796175.471		-197.1714	-0.728563	376.03665		-0.419729
	B(3)	58.4184	84.8615	49279.63198		-50.3818	-0.877089	84.86155		0.326972
	N(4)	-55.9025	320.7669	2411944.05		-210.7221	-0.985182	320.76685		-0.471104
	C(5)	88.4921	44.0014	631541.8708		-24.5579	-0.8055	44.0014		0.39646
	N(6)	179.4346	98.5292	5284275.304		-36.6373	-0.207122	98.5292		-0.484981
	B(7)	43.7014	110.2356	-34017.87152		-55.7705	-0.682273	110.23555		0.412679
	N(8)	162.3546	71.9997	3941141.184		-48.838	0.9656722	-73.25705		-0.567943
	C(9)	162.552	23.3408	4263645.868		-12.1655	-0.720932	23.34075		-0.316321
	B(10)	46.8112	102.5661	-35327.87243		-57.0937	-0.802363	102.56615		0.269088
B3LYP/6-31G**	C(11)	135.7845	38.859	2424939.465		-27.0353	0.9164574	-40.55295		-0.090565
	C(12)	162.5181	28.4365	4223267.852		-21.839	0.736128	-32.75855		-0.297114
	C(13)	176.7045	18.8909	5472798.477	-5968.29	-18.0231	0.3975343	-27.0346	6.0327	-0.456388
	C(14)	144.934	41.5366	2928946.997		-29.5741	0.8726588	-44.36105		-0.078853
	C(15)	146.126	31.3694	2971401.164		-36.6604	0.1409014	-54.99055		-0.440885
	B(16)	39.2309	95.7724	-87586.18327		-61.8682	-0.967996	95.7724		0.431603
	N(17)	97.9689	172.0317	78069.91612		-130.4677	0.7581026	-195.7016		-0.472015
	C(18)	129.395	34.751	2116867.422		-17.0867	-0.644133	34.75095		0.119259
	C(19)	62.8065	165.8855	-281940.1518		-96.3183	-0.851825	165.88555		-0.11194
	C(20)	62.7809	164.8303	-308354.0264		-97.9389	-0.878006	164.83025		-0.088127
	C(21)	62.7287	161.946	-308346.5392		-97.3764	-0.891271	161.946		-0.09028
	C(22)	61.1785	149.4602	-293821.1147		-94.0346	-0.940387	149.46025		-0.125006
	C(23)	55.503	167.9716	-203054.9943		-90.7642	-0.766242	167.97155		0.142861
	C(24)	56.8902	168.3857	-227377.5291		-92.8055	-0.790404	168.3857		-0.095331
	C(25)	113.1015	20.4078	1432239.456		-12.4053	-0.903275	20.4078		-0.095216
	C(26)	-5.0275	124.9154	-92771.48806		-103.3287	0.6118842	-154.993		0.484547

Table 3. Cont'd

N(27)	187.7145	108.6551	5957456.304	-43.9518	-0.351906	108.65505	-0.460897
C(28)	95.7209	47.7382	651667.6912	-52.7887	0.2057656	-79.18315	-0.006973
C(29)	-2.0427	105.8451	-86035.09052	-90.907	0.5524305	-136.3605	0.51879
N(30)	6.1919	237.0884	-1780486.224	-222.0534	0.4236116	-333.0801	-0.525142
C(31)	127.9014	35.0903	2036336.852	-21.2396	-0.898581	35.09035	-0.053969
C(32)	31.1638	86.6962	-311925.6197	-88.0667	0.3125835	-132.1	0.11527
C(33)	76.5929	116.3884	108722.2385	-65.786	-0.820538	116.38835	0.076192
C(34)	156.533	23.1207	3808315.873	-12.183	-0.734819	23.12065	-0.397289
S(35)	561.3809	176.1978	174450380.4	-70.9823	-0.345148	176.1978	0.131749
C(36)	165.5701	35.1701	4451617.911	-22.9749	-0.979469	35.1701	-0.373581
C(37)	26.3699	96.0474	-405040.7669	-99.3151	0.2894635	-148.9727	0.520486
O(38)	-175.0304	630.6477	34291881.83	-298.9932	-0.593842	630.6477	-0.366803
O(39)	102.7417	176.0419	-1485224.956	-161.1255	0.4567676	-241.6883	-0.490176
O(40)	-237.7739	722.1522	52748179.99	-351.5894	-0.630691	722.15215	-0.398075
O(41)	-382.483	1032.2281	143451314.9	-585.9808	-0.825641	1032.2282	-0.364674
N(42)	218.6694	60.6376	10210990.73	-25.5418	-0.417296	60.63755	-0.488341
C(43)	152.0439	28.7696	3476877.717	-16.1995	-0.816031	28.76965	-0.169595
C(44)	151.7475	34.7577	3422774.61	-20.4236	-0.86544	34.7577	-0.175195

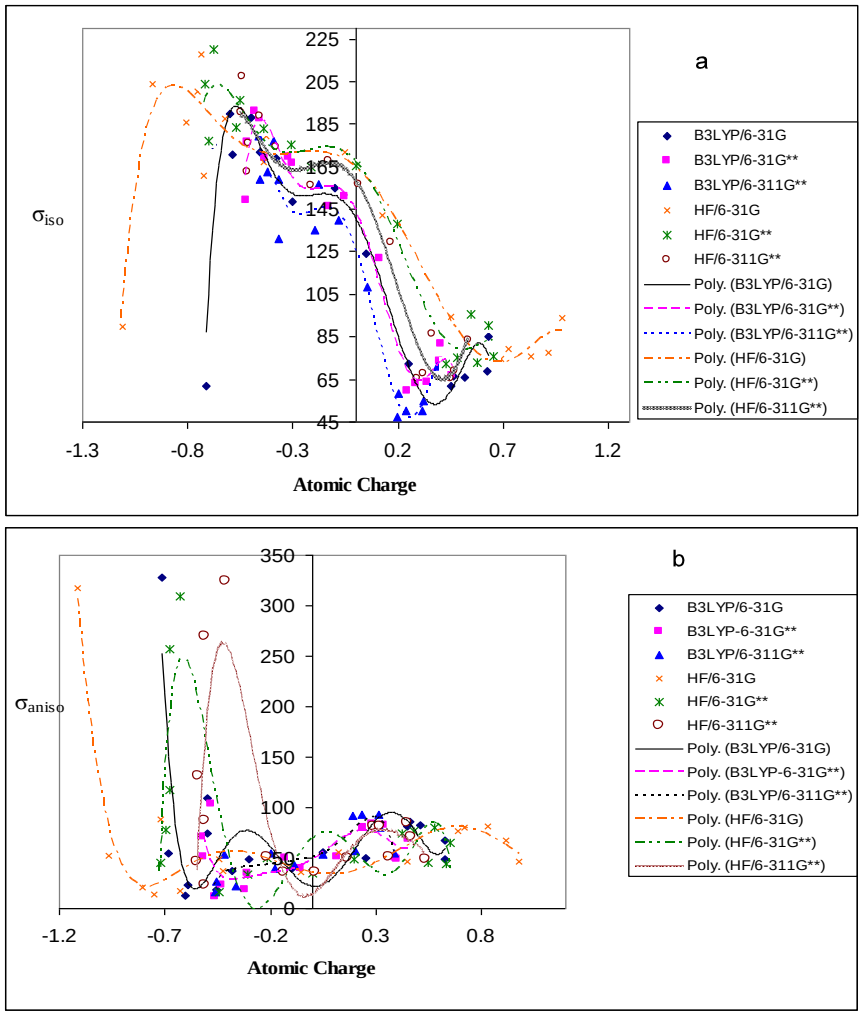

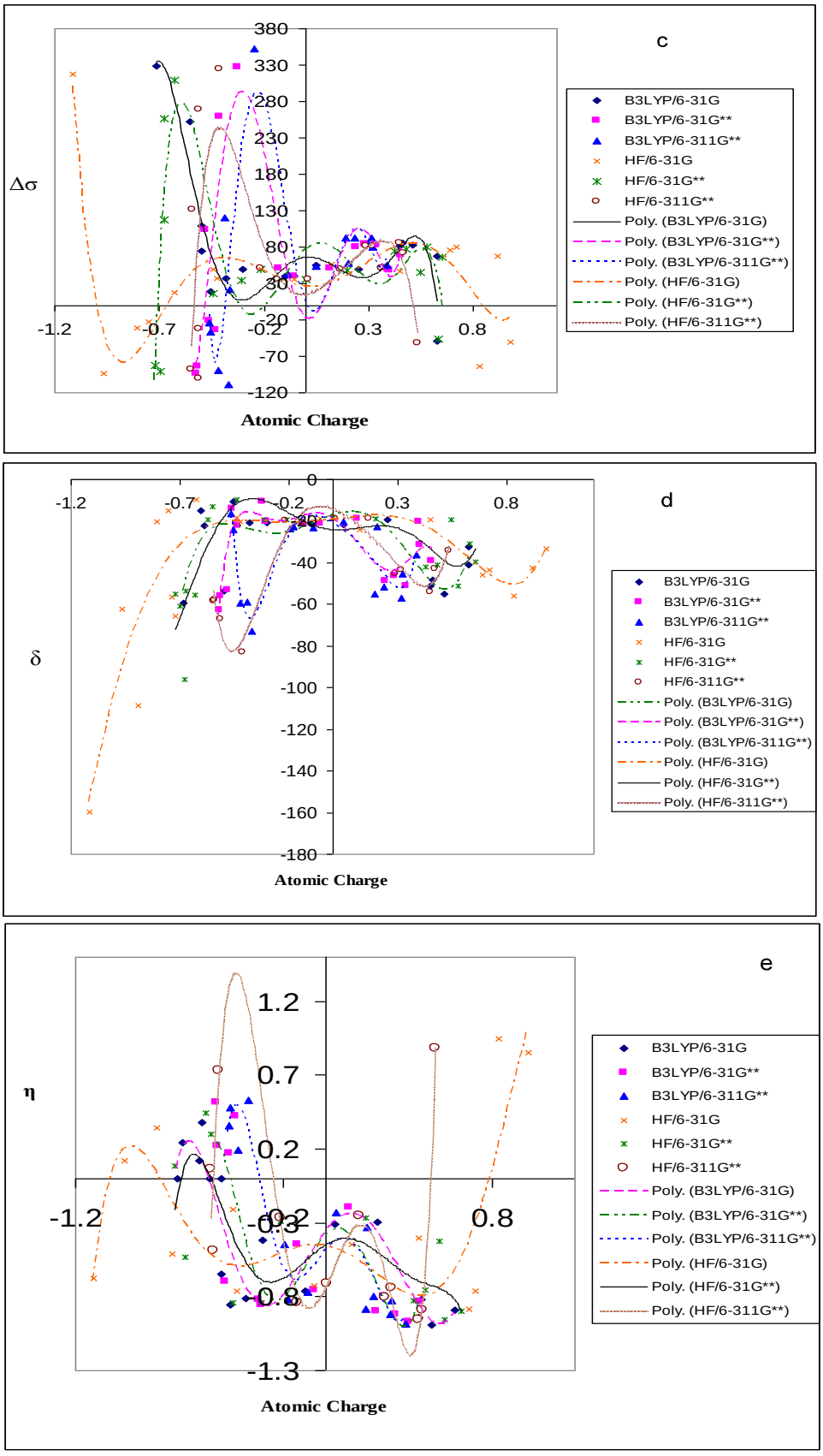

Figure 2. Plot of a) σiso b) σaniso c) Δσ d) δ and e) η versus atomic charge for $B_5N_5C_8H_{18}$ cluster.

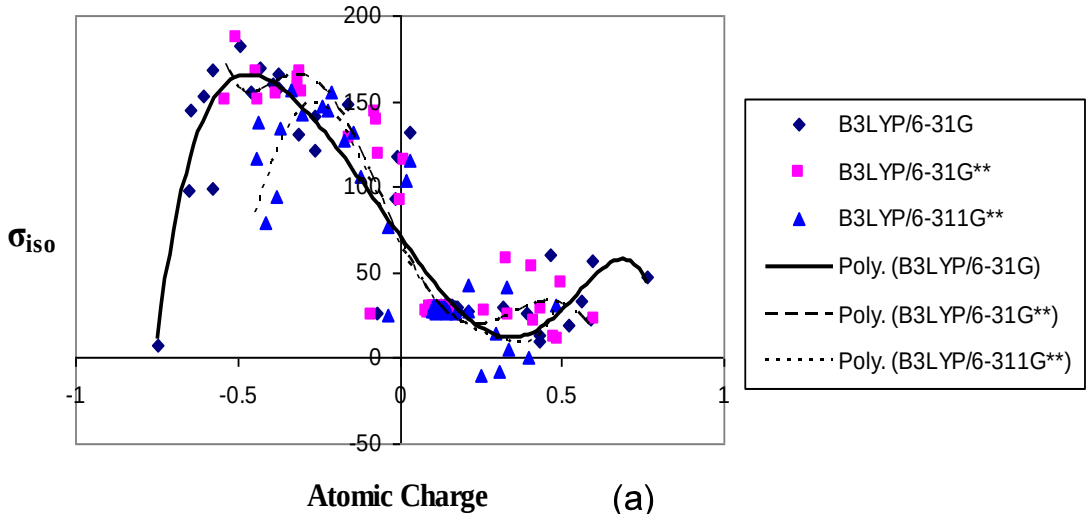
σiso
200
150
100
50
0
-50
-1
-0.5
0
0.5
1
B3LYP/6-31G
B3LYP/6-31G**
B3LYP/6-311G**
Poly. (B3LYP/6-31G)
Poly. (B3LYP/6-31G**)
Poly. (B3LYP/6-311G**)
Atomic Charge

(a)

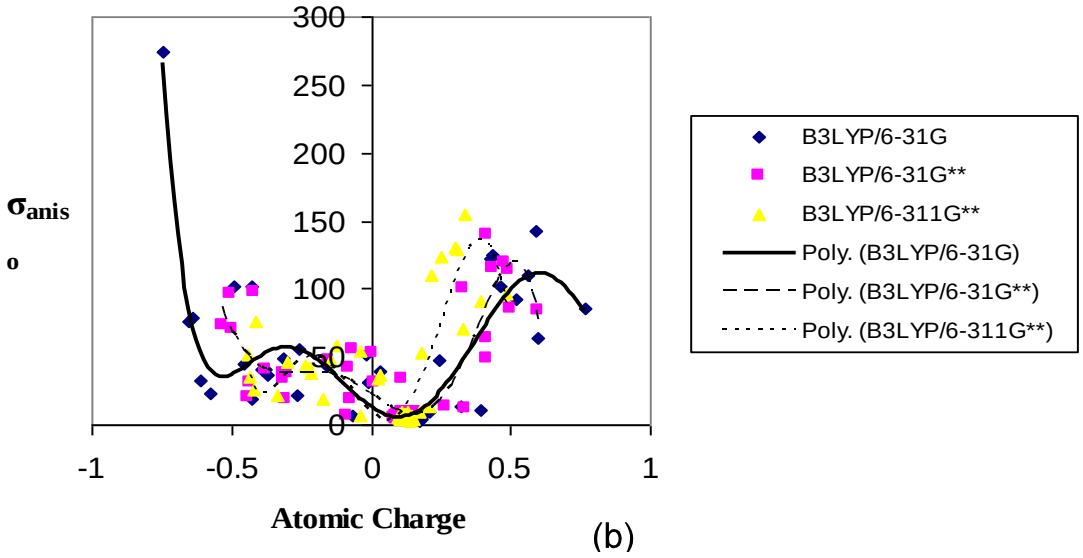
σanis
o
300
250
200
150
100
50
0
-1
-0.5
0
0.5
1
B3LYP/6-31G
B3LYP/6-31G**
B3LYP/6-311G**
Poly. (B3LYP/6-31G)
Poly. (B3LYP/6-31G**)
Poly. (B3LYP/6-311G**)
Atomic Charge

(b)

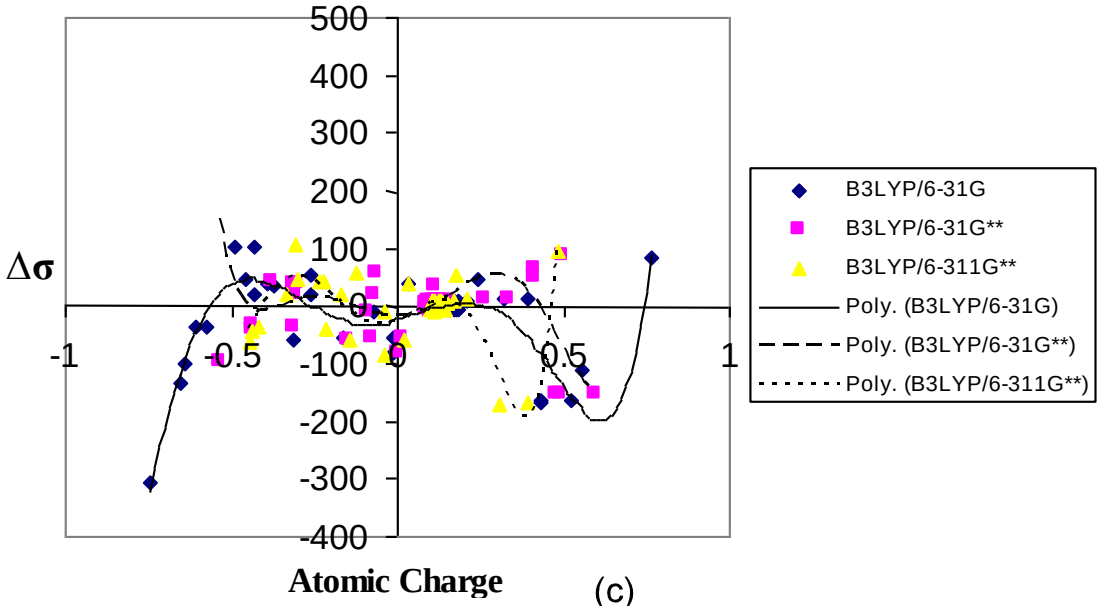
Δσ
500
400
300
200
100
0
-100
-200
-300
-400
-1
-0.5
0
0.5
1
B3LYP/6-31G
B3LYP/6-31G**
B3LYP/6-311G**
Poly. (B3LYP/6-31G)
Poly. (B3LYP/6-31G**)
Poly. (B3LYP/6-311G**)
Atomic Charge

(c)

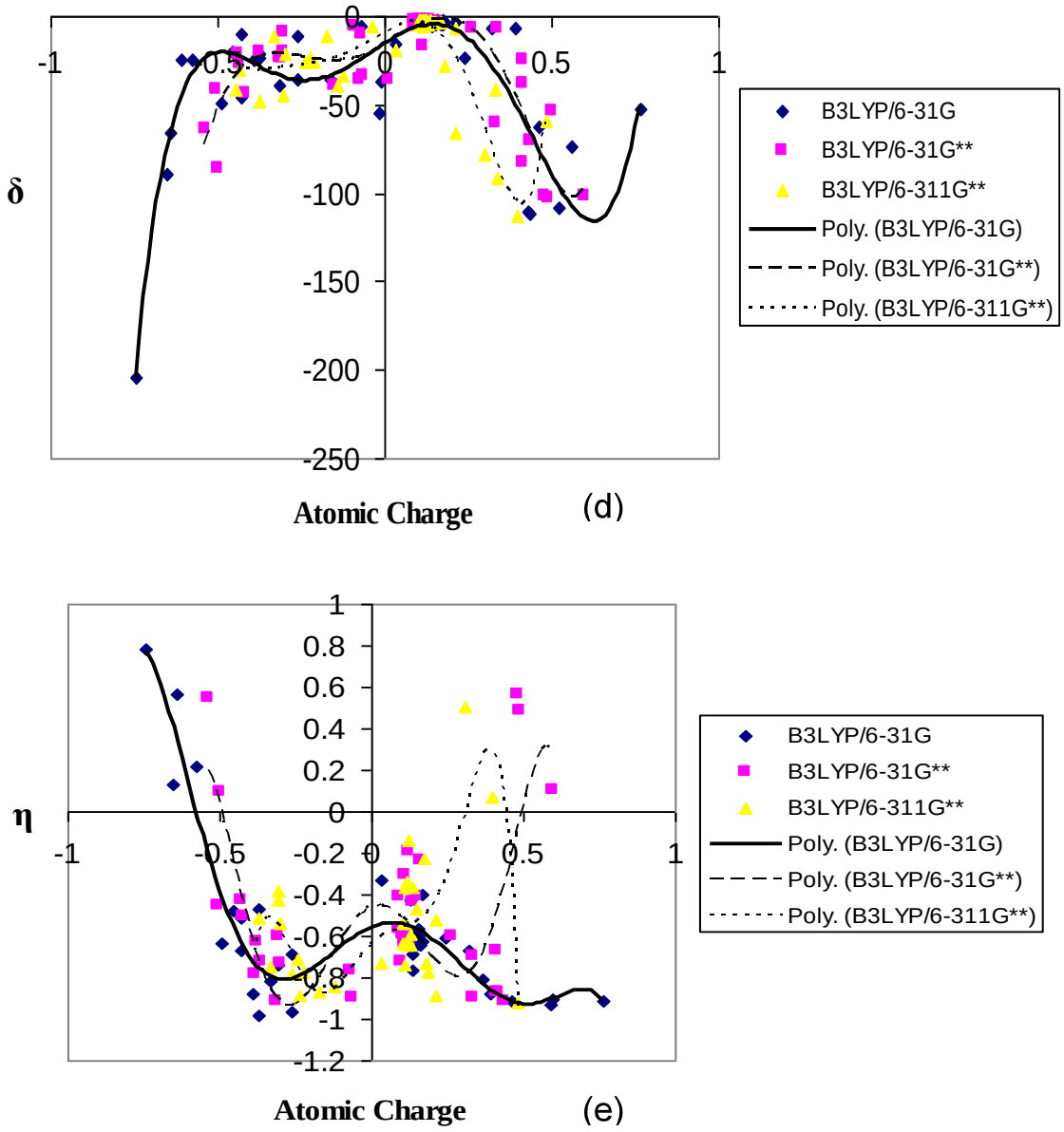

Figure 3. Plot of a) σiso b) σaniso c) Δσ d) δ and e) η versus atomic charge for penicillin inside $B_5N_5C_8H_{18}$ cluster.

for $B_5N_5C_8H_{18}$ and $B_5N_5C_8H_{18}$/antibiotic are plotted in Figures 2 to 4.

These curves are drawn for different levels and different basic sets. Generally, all curves are similar. All of them have a maximum around –0.8 and have a turning point around -0.3. Also all curves have a minimum around 0.2. These curves show that partial atomic charges have same behavior on the magnetic shielding of atoms.

These curves show that the NMR System is very sensitive to partial atomic charges. Maximum points change between -0.9 to -0.7.

So we can find that most chemical shielding is between -0.9 to -0.7. Milestone converts into convexity in the concavity point. The concavity points are created due to the change of negative charge into a positive charge. These curves show that the mechanism of positive charge is different from negative charge. Positive and negative areas are completely different. The lowest magnetic shielding is observed near the point of 0.2.

Discussion on a σ_{aniso} and σ_{iso} curves are alike. There is a main different between σ_{aniso} and σ_{iso} curves.

In a σ_{iso} curve maximum is around -0.8 but in σ_{aniso} curve minimum is around -0.8. This is also predictable and shows that these curves are very sensitive. On the σ_{aniso} curve in the positive area anomalies are observed.

So the study of a positive area for this curve can not be beneficial. Therefore it is better we focus on studying δ

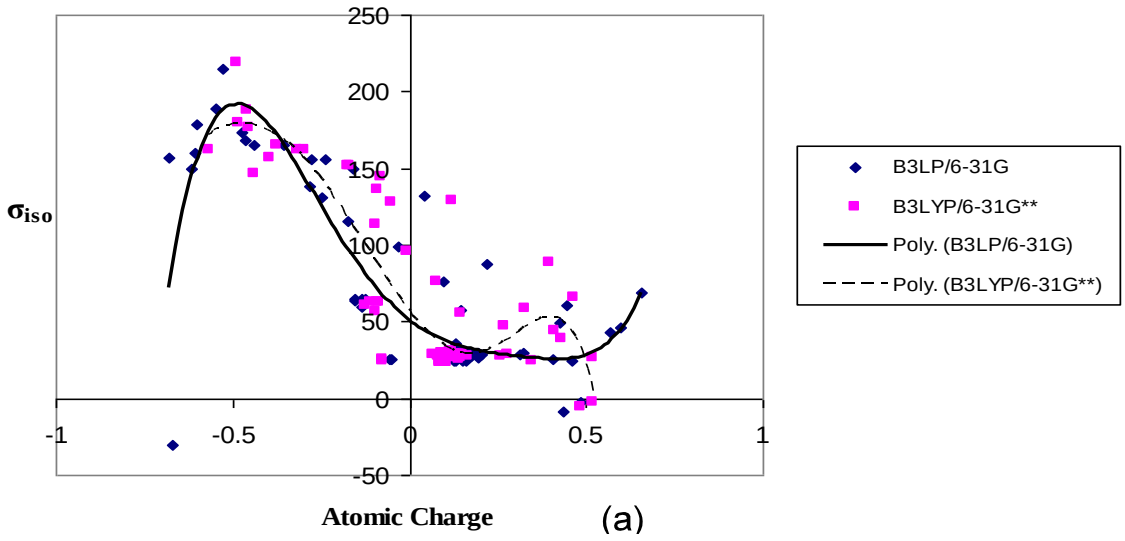
σiso
250
200
150
100
50
0
-50
-1
-0.5
0
0.5
1
Atomic Charge
B3LP/6-31G
B3LYP/6-31G**
Poly. (B3LP/6-31G)
Poly. (B3LYP/6-31G**)

(a)

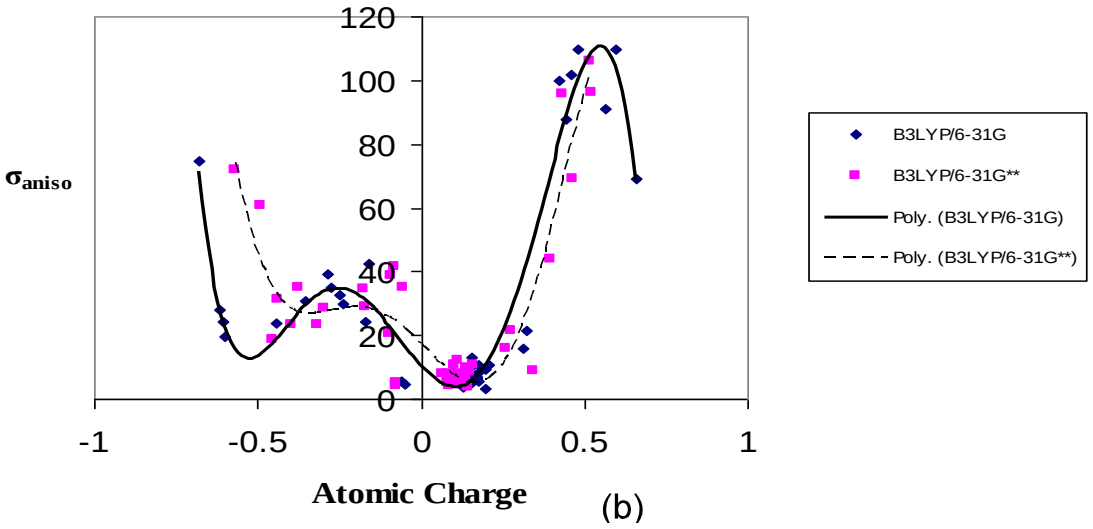
σaniso
120
100
80
60
40
20
0
-1
-0.5
0
0.5
1
Atomic Charge
B3LYP/6-31G
B3LYP/6-31G**
Poly. (B3LYP/6-31G)
Poly. (B3LYP/6-31G**)

(b)

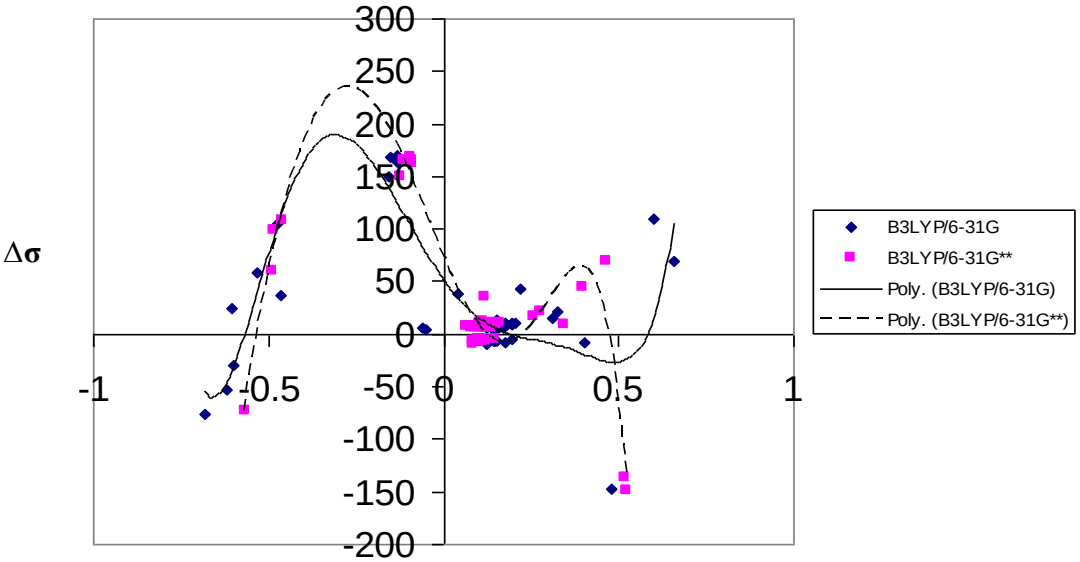
Δσ
300
250
200
150
100
50
0
-50
-100
-150
-200
-1
-0.5
0
0.5
1
Atomic Charge
B3LYP/6-31G
B3LYP/6-31G**
Poly. (B3LYP/6-31G)
Poly. (B3LYP/6-31G**)

(c)

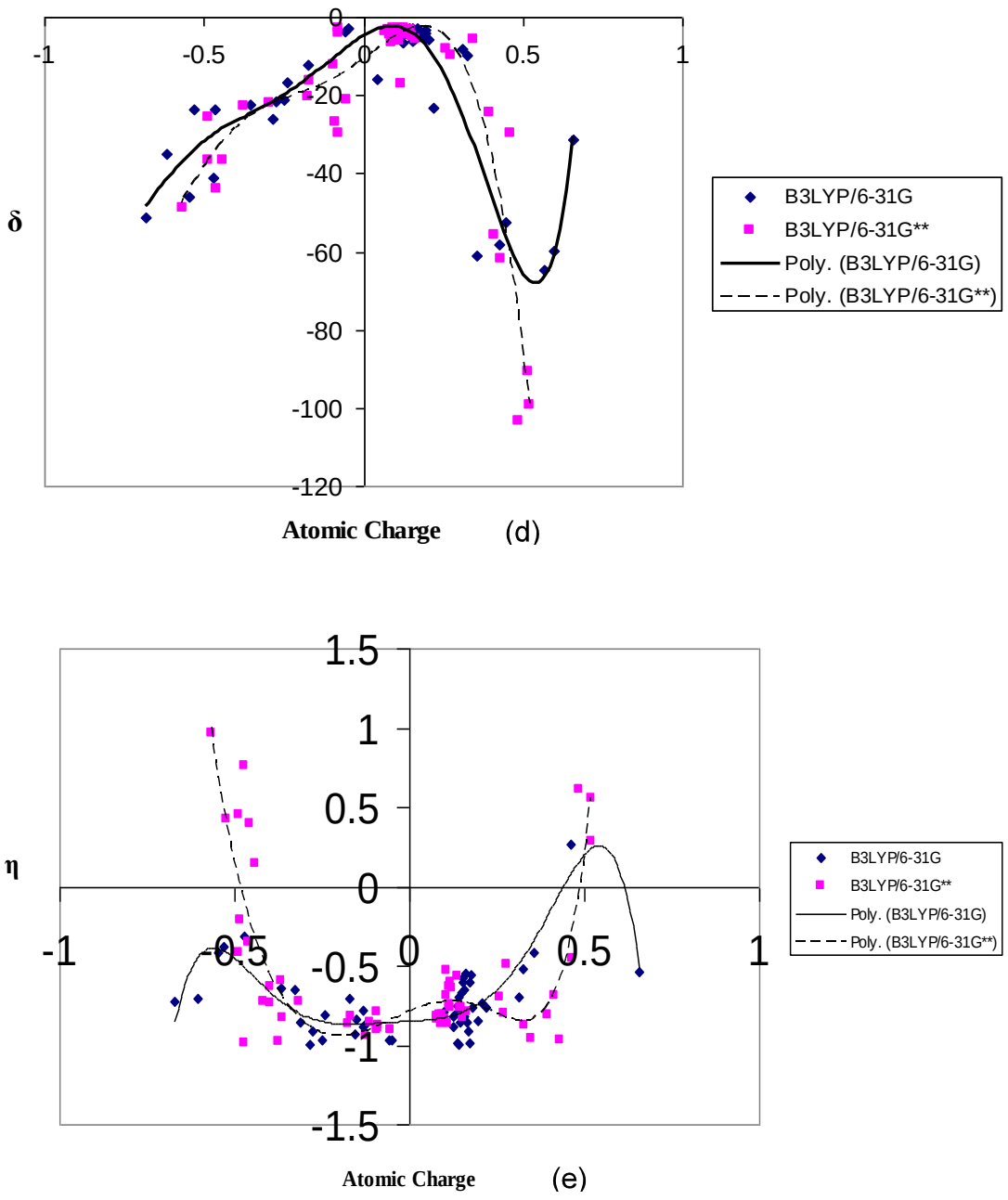

Figure 4. Plot of a) σiso b) σaniso c) Δσ d) δ and e) η versus atomic charge for cefalexin inside $B_5N_5C_8H_{18}$ cluster.

and η. δ and η are the results of σ_{iso} and σ_{aniso}. The curves in the negative and positive areas become more regular by connecting Penicillin. The results show penicillin is more sensitive than cefalexin to changing method. The maximum of σ_{iso} curve shift to the smaller negative value by connecting drug. In the σ_{aniso} curve, the change is in maximum rather than minimum points and also δ and η curves have a similar behavior.

The results show that antibiotics connect stronger to $B_5N_5C_8H_{18}$ cluster in negative charges than positive charge. Thus by creating negative field, antibiotics can be connected to the $B_5N_5C_8H_{18}$ cluster and delivered easily by using a positive filed. So $B_5N_5C_8H_{18}$ is a novel material for drug delivery.

REFERENCES

Azevedo S (2006). Energetic stability of B–C–N monolayer. Physics Letters A., 351: 109-112.
Behrman EC, Foehrweiser RK, Myers JR, French BR, Zandler ME

(1994). Possibility of stable spheroid molecules of ZnO. Phys. Rev. A., 49: R1543-R1546.
Curl RF, Smalley RE (1988). Probing C60. Sci., 242: 1017-1022.
Deepak FL, Vinod CP, Mukhopadhyay K, Govindaraj A, Rao CNR (2002). Boron nitride nanotubes and nanowires. Chemical Physics Letters, 353: 345-352.
Golberg D, Bando Y, Stephan O, Kurashima K (1998). Octahedral boron nitride fullerenes formed by electron beam irradiation. Appl. Phys. Lett., 73: 2441-2443.
Haubner R, Wilhelm M, Weissenbacher R, Lux B (2002). High Performance Non-Oxide Ceramics, Springer: New York, 102: 1-45.
Kar T, Pattanayak J, Scheiner S (2003). Rules for BN-Substitution in BCN-Fullerenes. Separation of BN and C Domains. J. Phys. Chem., 107: 8630–8637.
Kaxiras E, Jackson K, Pederson MR (1994). Theoretical study of passivated small fullerenes C24X4 (X=N, P, As) and their isoelectronic equivalents (BN)12X4. Chem. Phys. Lett., *225*: 448-453.
Kroto H (1988). Space, Stars, C60, and Soot. Sci., 242: 1139-1145.
Locke IW, Darwish AD, Kroto HW, Prassides K, Taylor R, Walton DRM (1994). Phosphorus/buckminsterfullerene intercalation compounds, C60(P4)2. Chem. Phys. Lett., 225: 186-190.
Loiseau A, Willaime F, Demoncy N, Schramchenko N, Hug G, Colliex C, Pascard H (1998). Boron nitride nanotubes. Carbon., 36: 743-752.
Monajjemi M, Chegini H, Mollaamin F, Farahani P (2011). Theoretical Studies of Solvent Effect on Normal Mode Analysis and Thermodynamic Properties of Zigzag (5, 0) Carbon Nanotube. Fullerenes, Nanotubes and Carbon Nanostructures,19: 469- 482.
Monajjemi M, Khaleghian M, Tadayonpour N, Mollaamin F (2010a). The effect of different solvents and temperatures on stability of single-walled carbon nanotube: a qm/md study. Int. J. Nanosci., 9: 517-529.
Monajjemi M, Lee VS, Khaleghian M, Honarparvar B, Mollaamin F (2010b). Theoretical Description of Electromagnetic Nonbonded Interactions of Radical, Cationic, and Anionic NH2BHNBHNH2 Inside of the B18N18 Nanoring. J. Phys. Chem. C ., 114: 15315–15330.
Monajjemi M, Mahdavian L, Mollaamin F (2008). Interaction of Na, Mg, Al, Si with Carbon Nanotube (CNT): NMR and IR Study1. Bull. Chem. Soc. Ethiop., 22: 1-10.
Monajjemi M, Mahdavian L, Mollaamin F, Khaleghian M (2009). Interaction of Na, Mg, Al, Si with Carbon Nanotube (CNT): NMR and IR Study1. Russian J. Inorg. Chem., 54: 1465-1473.
Moon WH, Hwang HJ (2004). Molecular mechanics of structural properties of boron nitride nanotubes. Physica E: Low-dimensional Systems and Nanostructures, 23: 26-30.
Mollaamin F, Gharibe S, Monajjemi M (2011). Synthesis of various nano and micro ZnSe morphologies by using hydrothermal method. Int. J. Phy. Sci., 6: 1496-1500.
Naruhiro K, Takeo O (2004). Hydrogen storage in boron nitride and carbon clusters studied by molecular orbital calculations. Solid State Commun., 131: 121–124.
Nirmala V, Kolandaivel P (2007). Structure and electronic properties of armchair boron nitride nanotubes. J. Molecular Structure: THEOCHEM., 817: 137-145.
Pokropivny VV, Skorokhod VV, Oleinik GS, Kurdyumov AV, Bartnitskaya TS, Pokropivny AV, Sisonyuk AG, Sheichenko DM (2000). Boron Nitride Analogs of Fullerenes (the Fulborenes), Nanotubes, and Fullerites (the Fulborenites). J. Solid State Chem., 154: 214-222.
Seifert G, Fowler PW, Mitchell D, Porezag D, Frauenheim TH (1997). Boron-nitrogen analogues of the fullerenes: electronic and structural properties. Chem. Phys. Lett., 268: 352-358.
Sun ML, Slanina Z, Lee SL (1995). Square/hexagon route towards the boron-nitrogen clusters. Chem. Phys. Lett., 233: 279-283.
Szakacs CE, Mezey PG (2008). Helices of Boron? Nitrogen Hexagons and Decagons. A Theoretical Study. J. Phys. Chem. A., 112: 6783-6787.
Takeo O, Atsushi N, Ichihito N (2004). Formation and atomic structures of BnNn (n=24–60) clusters studied by mass spectrometry, high-resolution electron microscopy and molecular orbital calculations. A Theoretical Study. Physica B., 351: 184-190.
Tang AC, Li OS, Liu CW, Li J (1993). Hückel treatment of carbon species with icosahedral symmetry. Chem. Phys. Lett., 201: 465-469.
Zhukovskii F, SergeiPiskunov N, Baiba B, Laima T, Stefano B (2009). Ab initio simulations on the atomic and electronic structure of single-walled BN nanotubes and nanoarches. J. Phys. Chem. Solids, 70: 796- 803.

‘